Remote Sensing of Clouds and Fog with a 1.4-mm Radar

JAMES B. MEAD, ROBERT E. MCINTOSH, DOUGLAS VANDEMARK* AND CALVIN T. SWIFT

Microwave Remote Sensing Laboratory, Department of Electrical and Computer Engineering, University of Massachusetts, Amherst, Massachusetts

31 October 1988 and 1 May 1989

ABSTRACT

A recently developed 1.4 mm wavelength incoherent radar has potential for remote sensing of low reflectivity atmospheric targets for ranges up to several kilometers. Power output of 60 W is achieved using an Extended Interaction Oscillator (EIO). Preliminary reflectivity measurements of clouds and fog for ranges between 36 and 1900 meters are believed to be the first such measurements at this wavelength. Limitations on the accuracy of the reflectivity measurements are discussed, highlighting uncertainties due to highly variable attenuation.

1. Introduction

To address the need for ever greater spatial resolution and sensitivity in the study of small-scale cloud processes, researchers are considering millimeter-wavelength radars operating in the atmospheric absorption windows centered at 8.6, 3.2, 2.1 and 1.4 mm. Recent advances in millimeter-wave technology have led to the development of commercially available high power linear beam tubes, solid state local oscillators and efficient receiver front ends operating in the frequency range of 30 to 300 GHz (1 cm–1 mm). Although propagation losses in dense clouds and rain are significant, these radars have enhanced sensitivity for particles below 100 μm while the high directivity available from relatively small antennas makes them attractive for airborne platforms. Lhermitte (1988) has demonstrated the ability of a portable 3.2 mm wavelength (94 GHz) radar to make measurements of vertical velocity of water and ice particles in fair weather cumulus, stratiform rain and high altitude cirrus (12–14 km). Lhermitte's radar employs a 1 kW peak power Extended Interaction Oscillator (EIO) and uses a COHO–STALO (coherent oscillator–stable local oscillator) technique to achieve phase coherence for Doppler.

The University of Massachusetts Microwave Remote Sensing Laboratory (MIRSL) has recently developed an incoherent 60 W peak-power, 1.4 mm wavelength (215 GHz) radar (McIntosh et al. 1988). The radar has sufficient sensitivity to detect -25 dBZ_e targets at a range of 1 km. Measurements of cloud and fog reflectivity were made for ranges between 36 and 1900 meters. To our knowledge these are the first such measurements made by a radar operating at this wavelength. Although the radar presented herein employs a transmitting tube similar to Lhermitte's, it has lower output power due to its higher operating frequency. The increased scattering efficiency at 1.4 mm compared to 3.2 mm (14.4 dB) more than offsets the reduction in power (-12.2 dB). While in theory the COHO–STALO technique could be used to add phase coherence to this radar, we have not attempted to add this capability.

Atmospheric absorption due to water vapor and liquid water strongly affects the overall performance of any millimeter-wavelength radar. This is especially true in the 1.4 mm atmospheric window where water vapor attenuation can vary between 1 dB km^{-1} for cold, dry conditions to as much as 12 dB km^{-1} for hot, humid weather. Attenuation by liquid water can also be quite severe, varying between 1 dB km^{-1} for light rain to over 30 dB km^{-1} for a heavy downpour. In the data presented, we attempted to reduce errors due to water vapor absorption by estimating the water vapor profile from surface measurements. Correction of attenuation due to liquid water proved to be problematic. Estimates of liquid water attenuation from measured reflectivity values, assuming a hypothetical drop size distribution, proved to be highly sensitive to change in the postulated mode radius.

A summary of the radar system is given in section 2. The range capability of the radar is discussed in section 3, where consideration is given to atmospheric absorption due to water vapor and extinction and

* Present affiliation: McDonnell Douglas Helicopter, Mesa, Arizona.

Corresponding author address: Dr. Robert E. McIntosh, Department of Electrical and Computer Engineering, University of Massachusetts, Amherst, MA 01003.

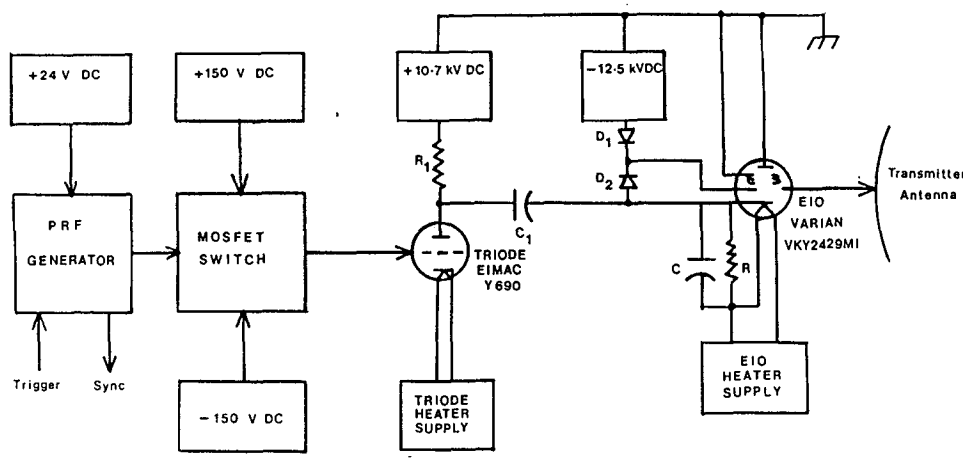

FIG. 1. Block diagram of radar transmitter.

backscattering by liquid water. Section 4 presents preliminary measurements that have been made to date, with a discussion of limitations of the data presented.

2. System description

A block diagram of the 1.4 mm radar system is given in Figs. 1 and 2. Table 1 summarizes the important parameters for estimating overall system performance. The transmitter employs a Varian VKY2429M1 EIO capable of producing 60 W pulses at a duty cycle up to 0.005. The modulator consists of an internal Pulse Repetition Frequency (PRF) generator, a Field Effect Transistor (FET) switch, and a high-voltage triode switch. The triode acts as a hard-tube modulator, that is capable of providing the high peak currents to rapidly charge the EIO stray capacitance, while providing a flat pulse to minimize EIO frequency drift. The receiver front end employs a single-ended mixer driven by a 71.2 GHz InP Gunn diode local oscillator through a frequency tripler. The double sideband (DSB) noise figure of the mixer subsystem is 10 dB. An automatic frequency control (AFC) loop operating between 1.2 and 1.6 GHz down-converts the signal to 160 MHz, where a logarithmic amplifier is used prior to detection. Separate 6-inch Gaussian optics lens antennas with scalar feed horns are used to achieve high isolation (>100 dB) between transmitter and receiver. A dual antenna scheme was chosen due to inefficiency of circulators and transmit/receive switches at this wavelength.

3. Range evaluation

a. *Water vapor absorption*

Propagation at a wavelength of 1.4 mm is limited by water vapor absorption, as well as attenuation due to liquid water. Attenuation due to O_2 is negligible, having a value of about 0.02 dB km^{-1} at sea level at 15°C. Improved algorithms have been developed (Liebe 1985) to predict water vapor attenuation for frequencies between 1 and 1000 GHz. Figure 3 plots attenuation, L_w, (in dB km^{-1}) due to water vapor versus relative humidity at various temperatures for λ = 1.4 mm. Attenuation at λ = 3.2 mm is given for

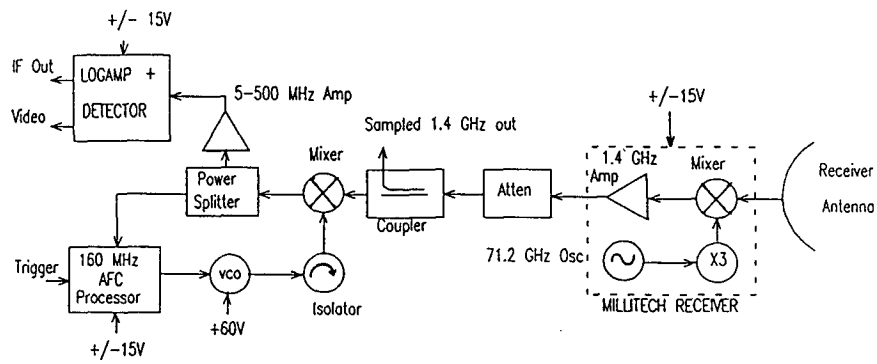

FIG. 2. Block diagram of radar receiver.

TABLE 1. Characteristics of UMass 1.4 mm wavelength radar system.

Transmitter	
Center frequency	215 GHz nominal
Peak output power	60 W
Pulsewidth	100–500 nsec
PRF	700 Hz–20 KHz
Tuning bandwidth	300 MHz
Max duty cycle	0.005
Antenna	
	6″ Lens
3 dB beamwidth	0.64 deg
Gain	48 dB
Receiver	
Noise figure	10 dB DSB
1st IF	1.4 GHz
2nd IF	160 MHz
Bandwidth	Variable, 5–40 MHz
Dynamic range	70 dB

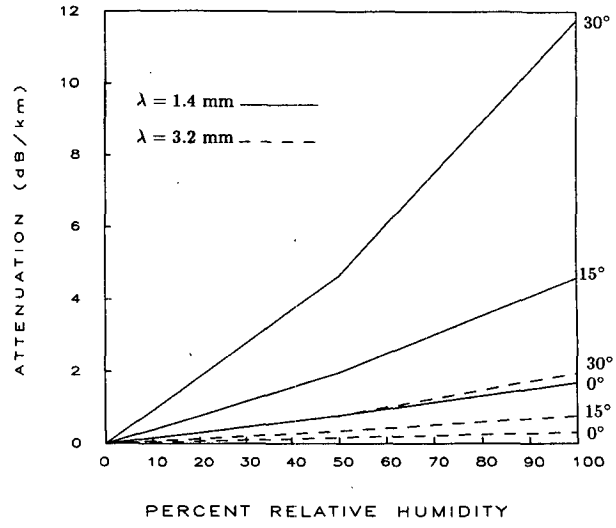

FIG. 3. Attenuation, L_w, of atmosphere due to water vapor at λ = 1.4 and 3.2 mm as a function of temperature. Atmospheric pressure is 1013 mb.

comparison. Water vapor density, ρ_v, may be modeled as a function of altitude by $\rho_v(z) = \rho_0 e^{-z/H}$ where H is the scale height, which is approximately 2.25 km (Ulaby et al. 1981; p. 264), and ρ_0 is the surface water vapor density in g m^{-3}. Since L_w depends linearly on ρ_v to a first order, $L(z)$ may be found from Fig. 3 by

$$L_w(z) = L_w e^{-z(\text{km})/2.25}. \quad (1)$$

Thus, at an altitude of 5 km, water vapor absorption will be reduced by an order of magnitude.

b. *Scattering and extinction by liquid water*

Backscatter and attenuation due to water droplets may be modeled using the Mie solution for scattering by dielectric spheres (Mie 1908; Ulaby et al. 1981). Spheres smaller than 112 μm (0.08λ) are more easily modeled using Rayleigh scattering (Ulaby et al. 1981). Two parameters of interest are the extinction coefficient, K_e, in dB km^{-1}, and the volume backscattering coefficient, η, in m^2 m^{-3}. Using an approximate drop size distribution and applying the Mie solution, K_e and η have been computed for several representative clouds and rain. Reflectivity values for meteorological targets measured with millimeter-wavelength radars are often reported using the equivalent reflectivity factor, Z_e, to indicate non-Rayleigh scattering for large droplets. Here $Z_e = \eta\lambda^4/(\pi^5|K|^2)$, where $K = (m^2 - 1)/(m^2 + 2)$, and m is the complex index of refraction of water. At λ = 1.4 mm, $|K| = 0.816$ at 20°C. Lhermitte (1987) reports that Z_e will not exceed +30 dBZ_e at 3.2 mm wavelength, even in heavy rain. At 1.4 mm we compute an equivalent reflectivity of +13 dBZ_e for 100 mm h^{-1} rain, showing very strong saturation of the Z–R relationship. Table 2 summarizes reflectivity and attenuation computations for various cloud and rain models. Distribution parameters α and γ (Colwell 1983) for the modified gamma function (Deirmendjian 1969) are given for the cloud examples. The modified gamma function takes the form

$$p(r) = ar^\alpha \exp(-br^\gamma)$$

TABLE 2. Extinction coefficient, K_e, and volume backscattering coefficient, η, for selected cloud types at 1.4 mm.

Cloud/rain description	Distribution parameters: Liquid water (g m^{-3})	Mode radius (μm)	α	γ	Extinction K_e (dB km^{-1})	Backscatter η [(dB m^{-1})/dBZ_e]
Stratocumulus	0.25	10.0	6.0	0.5	2.8	−51/−8
Low-lying stratus	0.25	10.0	6.0	1.0	2.6	−59/−16
Fog layer	0.15	20.0	7.0	2.0	1.6	−57/−14
Cumulus congestus	0.80	20.0	5.0	0.3	22.5	−28/+15
Rain 1 mm h^{-1}		Laws–Parsons			1.4	−42/+1
Rain 25.4 mm h^{-1}		Laws–Parsons			10.5	−34/+9

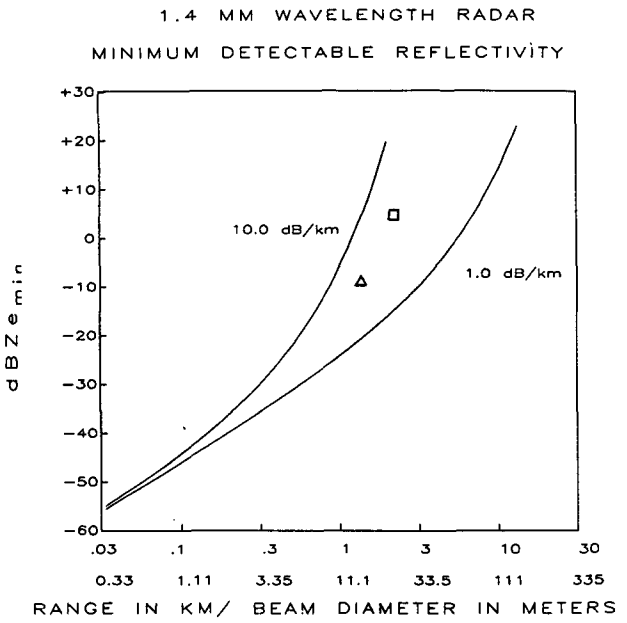

FIG. 4. Minimum detectable reflectivity versus range, assuming integration of 2000 pulses. Also shown is beam cross-sectional diameter for various ranges. Maximum penetration into stratocumulus (△) and 1 mm h^{-1} rain (□) are also given, assuming L_w = 4 dB km^{-1}.

where r is drop radius, and a and b are functions of α, γ, liquid water content and mode radius.

The received power scattered from volume targets is given by the radar range equation (Nathanson 1969):

$$P_r = \frac{P_t G^2 \lambda_0^2 c\tau \phi^2 \eta 10^{2L_a R/10\,000} L_t L_r}{1024 \ln(2) \pi^2 R^2} \qquad (2)$$

where R is the scattering cell range in meters, $c\tau$ is 120 meters (τ = 400 ns pulse), λ_0 = 0.0014 m, ϕ is the antenna beamwidth = 0.01117 rad, P_t is the peak transmitted power = 60 W, G is the antenna gain = 48 dB, L_a is total atmospheric loss in dB km^{-1} found by adding loss due to water vapor and loss from liquid water, and L_t and L_r are the transmitter and receiver losses $\approx$ 0.8. Equation (2) may be solved for $\eta_{\min}$, given the minimum detectable signal for 0 dB S/N, $P_{r_{\min}} = -91$ dBm. Converting $\eta_{\min}$ to Z_e in logarithmic form gives

$$\mathrm{dB}Z_{e_{\min}} = 20 \log R + \frac{L_a R}{500} - 74.7 \qquad (3)$$

which assumes that single radar pulses are being detected with no integration gain.

Practical measurements involve temporally and spatially averaging many pulse returns to reduce the variance in the estimate of reflectivity and to reduce the effective receiver noise level. For incoherent measurements, the variance is reduced by M, where M is the effective number of independent samples of the target which depends on signal decorrelation time, while the noise floor is reduced by $N^{1/2}$, where N is the number of averaged samples. An estimate of the signal decorrelation time for fog data (see below) was made by computing the normalized autocovariance of the backscattered power $C(\tau)$. The e^{-1} point of $C(\tau)$ occurred for $\tau \approx 800$ μs. Thus, for a sampling rate (PRF) below 1250 Hz, adjacent power samples should be essentially uncorrelated. For the measurements discussed below, we selected a PRF of 750 Hz, therefore $M \approx N$. An integration period of 2.6 seconds was used (N = 2000) which effectively lowers the noise floor by 16.5 dB. To ensure a high probability of detection (98%), however, a threshold was set 5 dB above the mean noise floor, giving a net improvement of 16.5 − 5 = 11.5 dB over the minimum reflectivity predicted by (3). Minimum dBZ_e, assuming 11.5 dB of integration gain is plotted in Fig. 4 versus range for total atmospheric loss = $K_e + L_w$ of 1.0 and 10.0 dB km^{-1}. The expected penetration depths for light rain and stratocumulus are also shown, using the values of K_e and dBZ_e given in Table 2, and L_w = 4 dB km^{-1}. Cross-sectional beam diameter is given along the abscissa as a function of range.

4. Measurements and discussion

Figure 5 shows the experimental setup used during May 1988 to evaluate the radar's ability to detect rain and clouds. The radar, which was housed in a garage, was aimed at a reflector plate to direct the beam vertically. Surface water vapor and temperature were

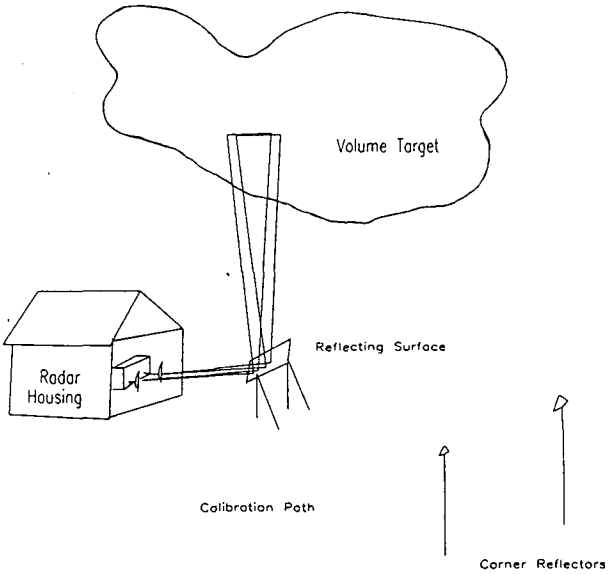

FIG. 5. Zenith profiling mode.

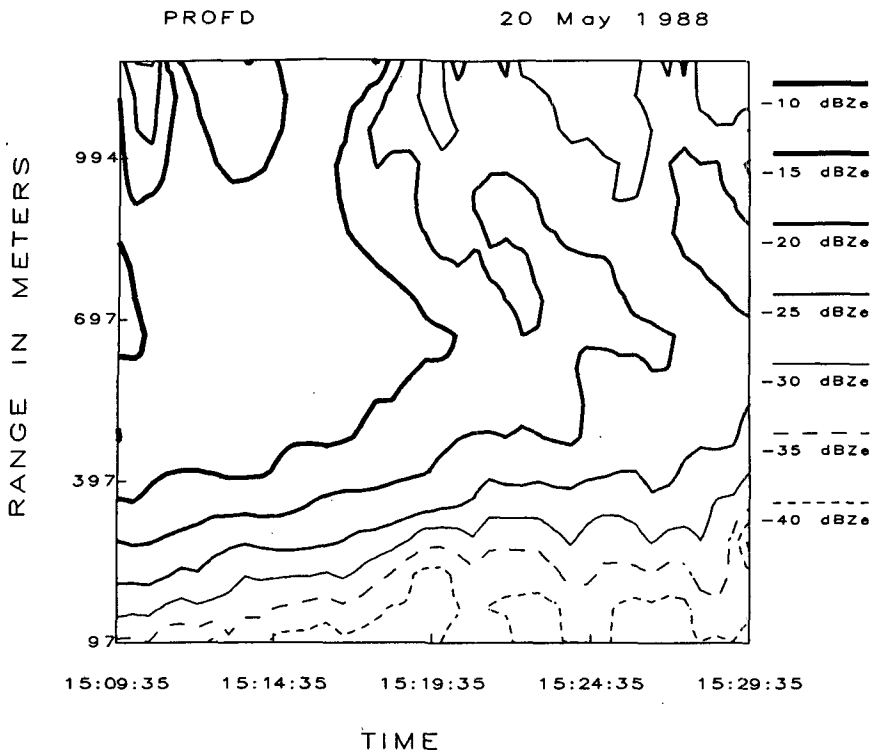

FIG. 6. Vertical profile of heavy stratocumulus reflectivity.

measured using a Weathertronics model 5165-A meter and were used to estimate L_w. Total attenuation at an altitude h was computed by integrating (1) from 0 to h and was used to correct the reported values of dBZ_e.

Figure 6 shows a contour plot of reflectivity versus altitude for a layer of heavy stratocumulus clouds. Note that the reflectivity at the starting observation time (15 h, 9 min, 35 sec) increases from roughly −35 dBZ_e at

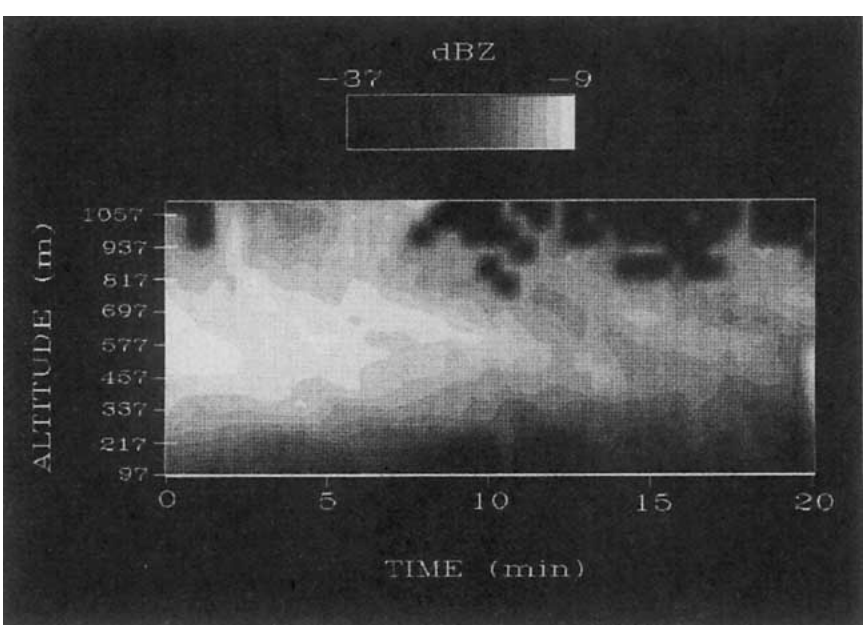

FIG. 7. Image of stratocumulus reflectivity.

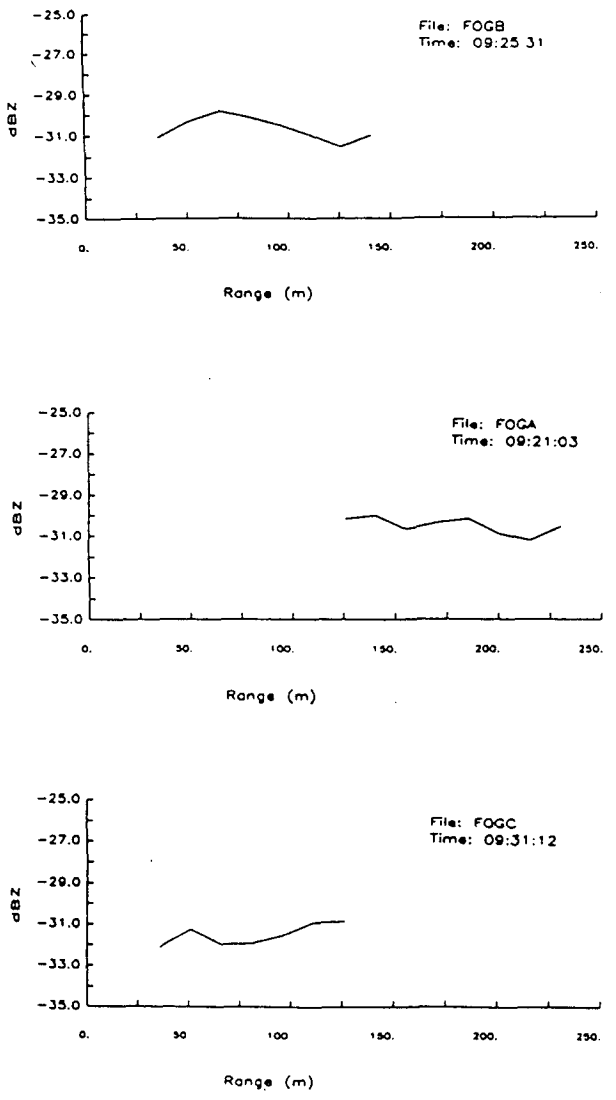

FIG. 8. Radar reflectivities obtained from fog measurements on 6 October 1987.

97 meters to approximately -12 dBZ_e between 400 and 800 meters then falls below -15 dBZ_e above 1000 meters. For the next 20 minutes the reflectivity at 97 meters fell steadily then leveled off at a value near -40 dBZ_e. At 600 meters, the reflectivity followed a similar trend, falling from its peak value of -10 dBZ_e to -23 dBZ_e at the 20-minute mark. An image of this cloud is also shown in Fig. 7.

Measurements of radiation (or inland) fog made on 6 October 1987 are shown in Fig. 8. These measurements were made from a 70-m high building in order to eliminate the effects of ground clutter. For these measurements, the pulse length was 100 ns and the receiver bandwidth was 12.5 MHz. Visibility during the measurements was approximately 100 m, which leads to an estimate of 0.08–0.12 g m^{-3} for liquid water content (Eldridge 1966). Since fog droplets typically range between 0.1 and 20 microns, we can use the Rayleigh approximation to compute absorption and estimate reflectivity, $Z \approx Z_e$. Using the standard formulation for liquid water absorption (Ulaby et al. 1981, p. 310)

$$Ke = (0.434)6\pi\lambda^{-1}\,\mathrm{Im}(-K)m_v \quad \text{in dB km}^{-1} \qquad (4)$$

and Atlas' (1964) approximation for reflectivity

$$Z_e \approx Z = 4.8 \times 10^{-2}\, m_v{}^2$$

we compute $Ke = 1$ dB km^{-1} and $Z = -35$ to -31.6 dBZ. The reflectivity values shown in Fig. 8 agree with the predicted result.

Since attenuation due to liquid water in nonprecipitating clouds can be on the order of several dB km^{-1}, we have attempted to estimate this loss based on the measured reflectivity values in order to correct the data. Although no precise relationship exists to compute extinction values from reflectivity, an estimate of this loss may be made by assuming a drop size distribution for the particular cloud being studied. Assuming a fixed mode radius, r_c, and distribution shape parameters γ and α, the liquid water content, m_v, may be estimated for a given reflectivity. Attenuation may then be approximated using (4). A drawback of this method is the strong dependence of the reflectivity on r_c in the Rayleigh region (30 dB/decade), leading to large errors in the estimate of m_v.

Figure 9a shows measured reflectivity for a low-altitude stratocumulus cloud corrected for liquid water attenuation using $r_c = 10$ μm, $\gamma = 0.05$, $\alpha = 6.0$. The same data, corrected for attenuation using $r_c = 15$ μm, $\gamma = 0.05$, and $\alpha = 6.0$, is shown in Fig. 9b. Note the significant change in contour shapes.

Figures 9a and 9b highlight the difficulty of making accurate reflectivity measurements using this radar as a stand-alone sensor in highly attenuating media. An accurate measure of m_v or attenuation is required to properly compensate the data. Direct measurement of attenuation could easily be achieved for ground-based measurements of fog using several calibration targets along the radar path. In a multisensor scheme, errors due to attenuation could be corrected by equating the average reflectivity within a given volume measured by the 1.4 mm wavelength radar to the value measured at a nonattenuating wavelength.

The feasibility of detecting clouds and fog with moderate sensitivity using a portable 1.4 mm wavelength radar has been demonstrated. Preliminary measurements at altitudes between 36 and 1900 meters have shown reasonable agreement with expected performance. Signal attenuation by water vapor and liquid water can add significant errors to measured values of reflectivity. A method for correcting errors due to at-

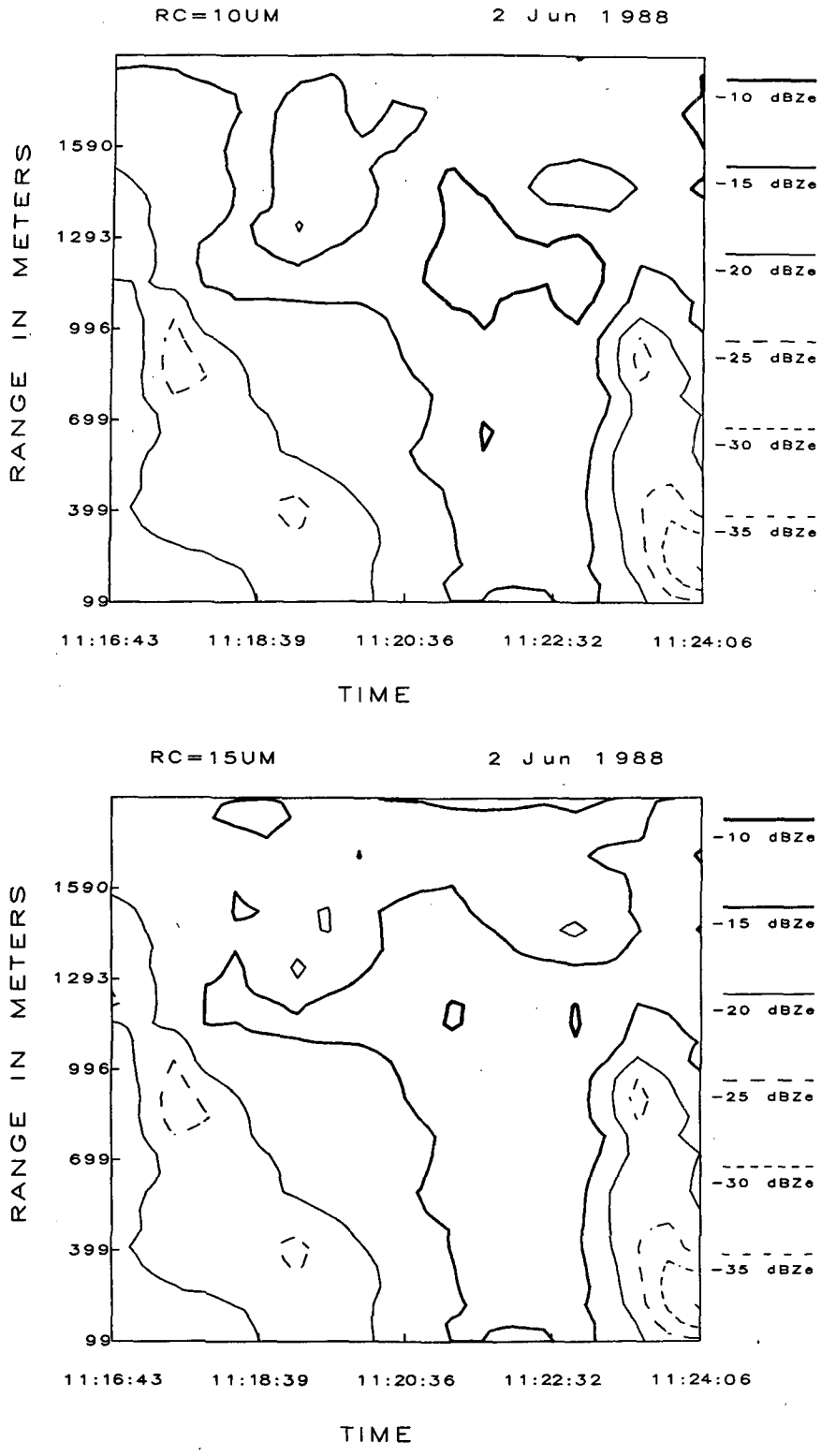

FIG. 9. Vertical profile of stratocumulus correcting for liquid water extinction, assuming (a) $r_c = 10$ μm and (b) $r_c = 15$ μm.

tenuation is necessary to improve the accuracy of such measurements.

REFERENCES

Atlas, D., 1964: Advances in radar meteorology, *Advances in Geophysics,* **10,** H. E. Landsberg and J. Van Miegham, Eds., Academic Press, 318–483.

Colwell, R. N. (Ed.), 1983: *Manual of Remote Sensing,* American Society of Photogrammetry, 196–197.

Deirmendjian, D., 1969: *Electromagnetic Scattering on Spherical Polydispersions,* Elsevier, 75–76.

Eldridge, R. G., 1966: Haze and fog aerosol distributions. *J. Atmos. Sci.,* **23,** 605–613.

Lhermitte, R. G., 1987: A 94 GHz Doppler radar for cloud observations. *J. Atmos. Oceanic Technol.,* **4,** 36–48.

——, 1988: Cloud and precipitation remote sensing at 94 GHz. *IEEE Trans. Geosci. Remote Sens.,* **26,** 207–216.

Liebe, H. J., 1985: An updated model for mm-wave propagation in moist air. *Radio Sci.,* **20,** 1069–1089.

McIntosh, R. E., R. M. Narayanan, J. B. Mead and D. H. Schaubert, 1988: Design and performance of a 215 GHz pulsed radar system. *IEEE Trans. Micro. Theory Tech.,* **36,** 994–1001.

Mie, G., 1908: Beitrage zur Optik trüber Medien, speziell Kolloidaler Metaläsungen. *Ann. Phys.,* **25,** 377.

Nathanson, F. E., 1969: *Radar Design Principles,* McGraw-Hill, 59–67.

Ulaby, F. T., R. K. Moore and A. K. Fung, 1981: *Microwave Remote Sensing, Active and Passive, Vol. I,* Addison-Wesley, 290–298.